Cardiovascular Research (2011) **89**, 374–383
doi:10.1093/cvr/cvq328

Cathepsin-L contributes to cardiac repair and remodelling post-infarction

Mei Sun[1], Manyin Chen[1], Youan Liu[1], Masahiro Fukuoka[1], Kim Zhou[2], Guohua Li[1], Fayez Dawood[1], Anthony Gramolini[3], and Peter P. Liu[1,4]*

[1]Division of Cardiology, Heart and Stroke/Richard Lewar Centre of Excellence, University Health Network, Toronto General Hospital, 200 Elizabeth Street, Toronto, ON, Canada; [2]McMaster University Medical School, Hamilton, ON, Canada; [3]Department of Physiology, CH Best Institute, Toronto, ON, Canada; and [4]Institute of Circulatory and Respiratory Health, Canadian Institutes of Health Research, NCSB 11-1266

Received 14 June 2010; revised 14 September 2010; accepted 11 October 2010; online publish-ahead-of-print 8 December 2010

Time for primary review: 27 days

Aims Cathepsin-L (CTSL) is a member of the lysozomal cysteine protease family, which participates in remodelling of various tissues. Herein, we sought to examine the potential regulation of CTSL in cardiac remodelling post-infarction.

Methods and results Experimental myocardial infarction (MI) was created in CTSL-deficient ($Ctsl^{-/-}$) mice (B6 × FSB/GnEi a/a $Ctsl^{fs}$/J) and wild-type littermates ($Ctsl^{+/+}$) by left coronary artery ligation. At days 3, 7, 14, and 28 post-MI, we monitored survival rate and evaluated cardiac function, morphology, and molecular endpoints of repair and remodelling. Survival was 56% in $Ctsl^{-/-}$ mice in contrast to 80% ($P < 0.05$) in $Ctsl^{+/+}$ mice post-MI by day 28. The $Ctsl^{-/-}$ mice exhibited greater scar dilatation, wall thinning, and worse cardiac dysfunction when compared with $Ctsl^{+/+}$ mice. Cardiac matrix metallopeptidase-9 (MMP-9) activity was also diminished, and *c-kit*-positive cells, natural killer cells, fibrocytes, and monocytes mobilized to peripheral blood and deposited to the infarcted myocardium were significantly decreased in $Ctsl^{-/-}$ mice. Furthermore, the local inflammatory response, and granulocyte-colony stimulating factor, stem cell factor (SCF), and stromal cell-derived factor-1 (SDF-1α) expression, as well as cell proliferation, revascularization, and myofibroblast deposition were significantly decreased *in* $Ctsl^{-/-}$ mice compared with $Ctsl^{+/+}$ mice.

Conclusion Our data indicate that CTSL regulates cardiac repair and remodelling post-MI through a mechanism with multiple pathways.

Keywords Angiogenesis • Cardiac remodelling • Cathepsin-L • Myocardial infarction

1. Introduction

Lysosomal cysteine proteases are ubiquitously expressed in different tissues and implicated in a variety of physiological and pathophysiological processes for their specific intra- and extracellular functions.[1,2] Lysosomal alterations and increased lysosomal enzyme activity in blood or tissues after myocardial ischaemia or infarction have been documented in patients.[3,4] Cathepsins belong to the papain-like family of lysosomal cysteine proteases,[5] which comprise 11 human and 19 murine enzymes.[6] Cathepsins participate in important biological functions, such as proteolytic processing of proenzymes, antigen presentation, extracellular matrix (ECM) and bone remodelling, cell invasion, tumour growth, and apoptosis.[7–10]

Cathepsin-L (CTSL) is known as a highly potent endoprotease of the cysteine cathepsin family. It is an ubiquitously expressed lysosomal enzyme, but has also been detected in the cytosol, nucleus,[11] and extracellular space.[12] Its multiple known diverse functions include the regulation of hair follicle cycling, epidermal homeostasis, major histocompatibility complex class II-mediated antigen presentation, tumour metastasis, and intracellular protein turnover.[13–16] Previous work has demonstrated that CTSL is required for endothelial progenitor cell (EPC)-induced neovascularization, and CTSL deficiency causes a significant impairment of blood flow restoration in ischaemic limbs.[17] Deficiency of CTSL in mice results in progressive dilated cardiomyopathy (DCM) and can be partially rescued by crossing transgenic CTSL into $Ctsl^{-/-}$ mice.[16,18,19]

After myocardial injury such as myocardial infarction (MI), extensive remodelling takes place both in the myocytes and ECM. Adverse remodelling can set the stage for ventricular dysfunction and heart failure. In the current study, we sought to determine the role of

* Corresponding author. Tel: +1 416 340 3035; fax: +1 416 340 4753, E-mail: peter.liu@utoronto.ca

CTSL in regulating and influencing cardiac repair/remodelling following injury using a well-established model of experimental MI[20,21] in *Ctsl*$^{-/-}$ and *Ctsl*$^{+/+}$ mice and to elucidate the potential underlying mechanisms.

2. Methods

2.1 Animals

All experiments using mice were approved by and performed according to the Guidelines for the Care and Use of Laboratory Animals in Toronto General University Health Network, which strictly conforms to the Guide for the Care and Use of Laboratory Animals published by the US National Institutes of Health (NIH Publication No. 85-23, revised 1996). Left ventricular (LV) MI was created in 8-week-old male *Ctsl*$^{-/-}$ and *Ctsl*$^{+/+}$ mice (B6 × FSB/GnEi a/a Ctsl^{fs}/J; Jackson Laboratory, ME) by left anterior descending coronary artery ligation as previously described by this laboratory[20] and for details, see Supplementary material online.

2.2 Evaluation of ischaemia risk zone by Evans blue perfusion

At 48 h post-MI, the hearts were perfused with 1% Evans blue dye and fixed with 10% formalin for 48 h. The hearts were sliced transversely from the apex to the base of the LV at 1 mm thickness each. The sections were captured with a Nikon digital camera for quantitative analysis of the area at risk and infarct zone.

2.3 Detection of CTSL enzyme activity

CTSL proteolytic activity was determined in tissue lysates (50 μg protein) by degradation of the fluoropeptide Z-Phe-Arg-4-methyl-coumarin-7-amide (20 μM; Bachem) in the presence of the CTSB-specific inhibitor CA074 (1.5 μM; Bachem) at pH 5.5. The release of 7-amino-4-methyl-coumarin was continuously monitored for 1 h by spectrofluorometry at excitation and emission wavelengths of 360 and 460 nm, respectively.

2.4 *In vivo* cardiac function measurements

Cardiac function was monitored non-invasively by echocardiographic imaging at 4 weeks after MI. Echocardiographic imaging was performed under light-controlled anaesthesia with isoflurane as previously described.[22] *In vivo* haemodynamic measurements were performed under light isoflurane anaesthesia in close-chested animals using a 1.4 French Millar catheter (Millar, Inc., Houston, TX, USA), and measurements were made as previously described.[23]

2.5 Cardiac morphometry

Morphometric analysis was performed on cardiac sections using a quantitative image digital analysis system (NIH image 1.6). Relative ventricular diameter, wall thickness, and infarct length were determined according to the method of Sun *et al.*[20]

2.6 Zymography

Protein was extracted with lysis buffer following homogenization. Samples (20 μg) were loaded onto each lane of 10% zymogram gelatin minigels (Novex, San Diego, CA). Gels were run at 35 mA for 2.5 h and then incubated in 2.5% Triton-X 100 for 2× 1 h at room temperature, washed, and further incubated for 16 h in 50 mmol Tris-HCl buffer, pH 7.5, containing 200 mmol NaCl and 10 mmol $CaCl_2$ at 37°C. Gels were stained for 90 min in Coomassie blue and destained in 30% methanol/10% acetic acid for 60 min. White bands on a blue background indicated zones of digestion corresponding to the presence of different matrix metallopeptidases (MMPs) identified on the basis of their molecular weight. Bands were scanned using a densitometer (GS-700; Bio-Rad, Hercules, CA). MMP levels were quantified using the Multianalyst software (Bio-Rad).

2.7 Flow cytometric analysis

The sample collection tube was rinsed with 50 μL heparin (1000 μL/mL). Blood samples (700–900 μL/mice) were collected from mice retro-orbital bleeding at baseline, and 3, 7, and 14 days after coronary artery ligation. Circulating cells were double-labelled with the following antibodies: phycoerythrin (PE)-conjugated CD11b and fluorescein isothiocyanate (FITC)-conjugated Gr-1 or biotin-conjugated anti-collage-I with Streptavidin-APC; FITC-conjugated c-Kit; PE-conjugated CD3 (BD Pharmingen), and FITC-conjugated NK1.1 (Bioscience). The cells were permeabilized with Cytofix/Cytoperm according to the manufacturer's instructions. The cells were examined by flow cytometry (BD FACS CaliburTM instrument and BD CellQuest^{TM} software) and analysed quantitatively (Flow Jo v8.5 software).

2.8 Immunohistochemistry

Cryostat sections (5 μm) were prepared, air-dried, and fixed in 4% paraformaldehyde/phosphate-buffered saline for 15 min. The sections were incubated with 0.3% hydrogen peroxide and 10% bovine serum albumin for 15 min. They were then incubated with antibody against Mac3, CD31 (BD Pharmingen Technical, Mississauga, ON), C-kit (Abcom, CA), alpha-smooth muscle actin (α-SMA) (Sigma, MO), and Ki-67 (Bethyl Laboratories, TX) at 4°C overnight. Finally, the sections were incubated with a matching biotinylated secondary antibody (Vector, Burlingame, CA) for 45 min at room temperature. Negative controls were performed for all immunologic staining by omission of the primary antibody.

2.9 Movat pentachrome staining

Cryostat sections (5 μm) were fixed in Bouin's solution for 30 min, followed by staining with Alcian Blue solution for 30 min. Slides were then washed in running water for 3 min and incubated with ammonium hydroxide in 95% alcohol (pH above 8) for 2 h. After washing with running water and rinsing in 70% alcohol, the slides were incubated with Weigert–Hart Resorcin solution for 3 h at 55°C and then stained with Weigert's haematoxylin for 15 min. Next, they were rinsed with running water and stained with Woodstain Scarlet Fuchsin solution for 5 min, followed by rinsing in 0.5% aqueous glacial acetic acid. Slides were then rinsed thoroughly in three changes of absolute alcohol and incubated with alcoholic saffron for 15 min. This was followed by washing with four changes of absolute alcohol. Finally, the slides were washed with several changes of xylene and then mounted in Permount.

2.10 Cardiac collagen volume fraction

Cardiac collagen volume fraction was determined in sections stained with Movat Pentachrome. The cardiac collagen volume fraction was calculated as the ratio of the sum of total interstitial collagen area to the sum of total collagen and non-collagen area in the entire visual field of the section as previously reported.[23]

2.11 Statistical analysis

Data are expressed as mean ± SEM. Differences among more than two groups were tested by one-way analysis of variance. Comparisons between two groups were performed by unpaired Student's *t*-test. A *P*-value less than 0.05 was considered significant.

3. Results

3.1 MI caused rapid CTSL activation in myocardium and bone marrow

The CTSL activity was significantly increased in the myocardium 24 h post-MI, peaking on day 3 in the ischaemic region. The activation of CTSL in the bone marrow followed a similar pattern, with CTSL

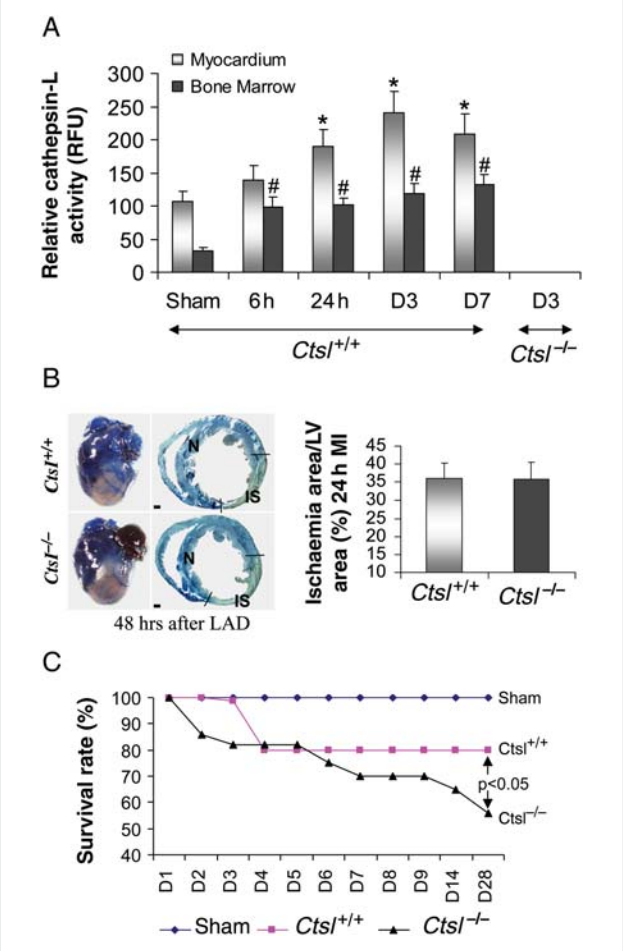

Figure 1 (*A*) Enhanced CTSL activity in myocardium and bone marrow in $Ctsl^{+/+}$ MI mice ($n = 4$). $^{*}P < 0.001$ vs. sham myocardium; $^{\#}P < 0.001$ vs. sham bone marrow. (*B*) Comparison of $Ctsl^{+/+}$ and $Ctsl^{-/-}$ infarct area in transversely sectioned heart excised at 48 h post-MI ($n = 3$) (blue: normal area, white: infarct area). Scale bars represented 100 μm. (C) Kaplan–Meier survival curves in $Ctsl^{+/+}$ ($n = 50$) and $Ctsl^{-/-}$ ($n = 75$) mice after MI. $^{*}P < 0.05$ vs. $Ctsl^{+/+}$ mice.

activity significantly increasing at 6 h post-MI and maintaining a stable level thereafter (*Figure 1A*). No CTSL activity was detected in $Ctsl^{-/-}$ mice.

3.2 CTSL deficiency predisposed to increased mortality at chronic phase after MI

The left anterior descending coronary artery ligation produced infarcts averaging $36 \pm 5.9\%$ of the LV wall in both $Ctsl^{+/+}$ and $Ctsl^{-/-}$ mice (*Figure 1B*). Survival rate after MI was compared between $Ctsl^{+/+}$ and $Ctsl^{-/-}$ mice using Kaplan–Meier statistics (*Figure 1C*). After 4 weeks of MI, the survival rate was significantly lower in $Ctsl^{-/-}$ mice (56%; 42 of 75) compared with $Ctsl^{+/+}$ mice (80%; 40 of 50, $P < 0.05$), whereas the sham-operated mice of either genotype all survived.

3.3 CTSL deficiency contributed to diminished function and adverse remodelling late post-MI

Following MI, anatomical and pathological examination of $Ctsl^{-/-}$ mice showed heart failure, as evidenced by pulmonary congestion and cardiac dilatation. M-mode echocardiography revealed exaggerated LV dilatation in $Ctsl^{-/-}$ mice at week 4 post-MI (*Table 1*). Invasive pressure–volume measurements demonstrated that LV end-systolic pressure was significantly decreased, whereas LV end-systolic (LVESV) and end-diastolic volume (LVEDV) were significantly increased in $Ctsl^{-/-}$ mice compared with $Ctsl^{+/+}$ mice ($P < 0.005$). Ejection fraction, positive d*P*/d*t*, and negative d*P*/d*t* were also significantly decreased in $Ctsl^{-/-}$ mice (Supplementary material online, *Figure S1*).

$Ctsl^{-/-}$ and $Ctsl^{+/+}$ mouse heart morphometry was assessed 28 days after MI (*Figure 2A*). LV diameter was significantly increased ($P < 0.001$) in the $Ctsl^{-/-}$ mice compared with $Ctsl^{+/+}$ mice (*Figure 2B*). Concomitantly, infarcted segment thickness was reduced ($P < 0.05$) in $Ctsl^{-/-}$ mice compared with $Ctsl^{+/+}$ mice (*Figure 2C*). We also evaluated the scar length as a percentage of the LV circumference by heart cross-section.[20] No difference was detected in scar length by day 7. $Ctsl^{+/+}$ mice showed a relative stabilization between day 7 and day 14, whereas $Ctsl^{-/-}$ mice showed continued infarct expansion (*Figure 2D*, $P < 0.001$) until day 28. Heart/body weight and lung/body weight ratios were increased in $Ctsl^{-/-}$ mice at day 28 (*Figure 2E* and *F*). Thus, impaired scar stability and progressive left ventricular dilatation after MI were likely contributing factors to the progression towards worsened cardiac dysfunction.

3.4 MMP-9 activation in myocardium and bone marrow correlated with CTSL activation post-MI

To elucidate the potential relationship between CTSL and MMP-9 activity (a major mediator of bone marrow cell mobilization), the timing of the MMP-9 expression patterns in the infarcted myocardium and bone marrow was analysed by zymography. As shown in *Figure 3*, MMP-9 activity was significantly increased in the infarcted heart at 6 h in the $Ctsl^{+/+}$ mice, reaching a peak at day 3, and decreasing thereafter. The sham group displayed very low levels of cardiac MMP-9, particularly in the $Ctsl^{-/-}$ mice. Although MMP-9 activity in the $Ctsl^{-/-}$ mice showed an increase, this was significantly diminished compared with $Ctsl^{+/+}$ mice at 6 and 24 h ($P < 0.001$; *Figure 3A*). Bone marrow MMP-9 activity rapidly increased in $Ctsl^{+/+}$ mice at 6 h and showed a delay of increase in $Ctsl^{-/-}$ mice. After 24 h, there was no statistical difference between the two groups (*Figure 3B*).

3.5 CTSL deficiency diminished peripheral blood and bone marrow cell response post-MI

The flow cytometric analysis of the peripheral blood was performed at 3 days post-MI. Analysis demonstrated that circulating cells with surface markers of $Gr\text{-}1^{+}/CD11b^{+}$ (monocytes), $C\text{-}kit^{+}$ (progenitor cells), $NK1.1^{+}/CD3^{+}$ (natural killer cells), and $CD11b^{+}/Collagen^{+}$ (fibrocytes) cells were all significantly lower ($P < 0.01$) in the $Ctsl^{-/-}$ mice when compared with those in the $Ctsl^{+/+}$ mice at 3 day post-MI (*Figure 3C* and Supplementary material online, *Figure S2*). However, these differences were no longer significant by days

Table 1 Echocardiographic data of 4 weeks after MI

	Ctsl$^{+/+}$		*Ctsl*$^{-/-}$	
HR (bpm)	526 ± 66.38	513 ± 66.25	534 ± 62	528 ± 52.59
FS (%)	44.92 ± 5.37	21.10 ± 3.01*	43.18 ± 3.18	11.16 ± 2.518†,*
PWD (mm)	0.61 ± 0.11	0.63 ± 0.085	0.64 ± 0.036	0.64 ± 0.091
IVSD (mm)	0.67 ± 0.11	0.63 ± 0.023	0.64 ± 0.04	0.65 ± 0.0293
LVESD (mm)	2.17 ± 0.41	4.3 ± 0.63*	2.21 ± 0.12	5.57 ± 0.66†,*
LVEDD (mm)	3.94 ± 0.47	5.45 ± 0.65*	3.89 ± 0.06	6.27 ± 0.65†,*
Number	5	10	5	10
Parameter	Sham	MI	Sham	MI

Two-dimensionally guided M-mode echocardiography was studied 4 weeks after MI.
LVEDD, left ventricle end-diastolic diameter; LVESD, left ventricle end-systolic diameter; IVSD, diastolic intraventricular septal thickness; PWD, diastolic posterior wall thickness; FS, fractional shortening; HR, heart rate.
*$P < 0.01$ for MI group vs. sham-operated mice.
†$P < 0.01$ for MI group of *Ctsl*$^{-/-}$ vs. *Ctsl*$^{+/+}$ mice.

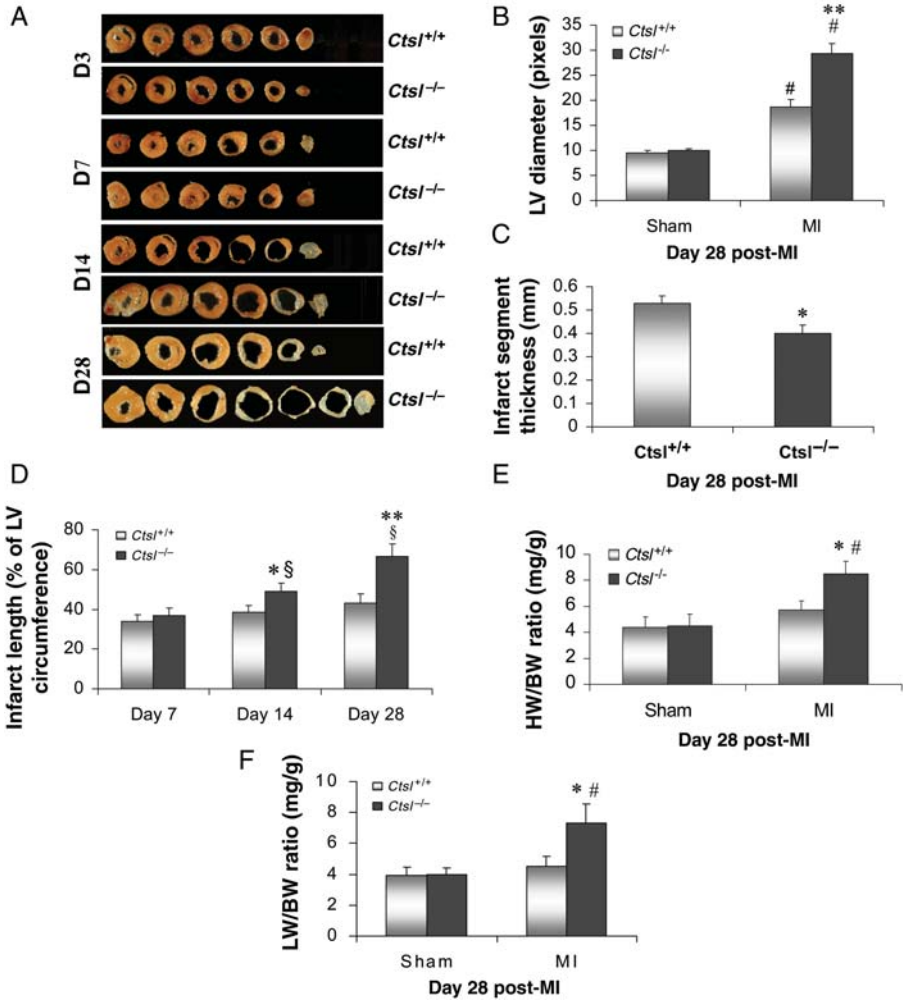

Figure 2 (*A*) Representative heart morphometry illustrations at 3, 7, 14, and 28 days after MI ($n = 5$); (*B*) Morphometric quantification in LV diameter, (*C*) infarct segment wall thickness, (*D*) percentage of infarcted/circumferential length, (*E*, *F*) heart/body and lung/body weight ratios in *Ctsl*$^{+/+}$ and *Ctsl*$^{-/-}$ mice at day 28 after MI ($n = 10$). **$P < 0.001$ vs. *Ctsl*$^{+/+}$ MI; *$P < 0.05$ vs. *Ctsl*$^{+/+}$ MI; §$P < 0.001$ vs. Day 7 groups; #$P < 0.001$ vs. sham groups.

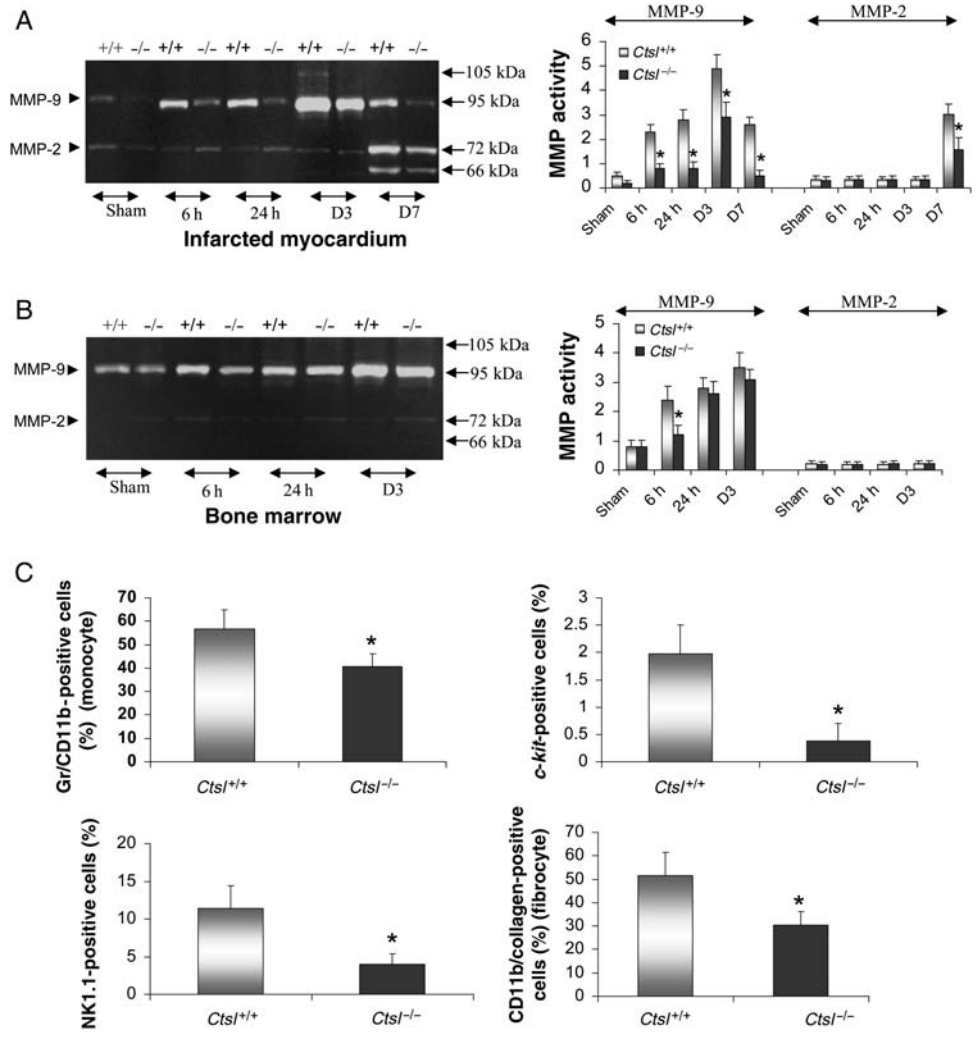

Figure 3 Representative MMP-9 activation in infarcted myocardium (*A*) and bone marrow (*B*) post-MI. $n = 5$ for each group; *$P < 0.001$ vs. $Ctsl^{+/+}$ MI mice. (*C*) Flow cytometry for $CD11b^{+}$/Gr-1^{+}, *c-kit*$^{+}$, $NK1.1^{+}$, and $CD11^{+}$/$Collagen^{+}$ cells from blood at day 3 post-MI in $Ctsl^{+/+}$ ($n = 5$) and $Ctsl^{-/-}$ ($n = 5$) mice. *$P < 0.01$ vs. $Ctsl^{+/+}$ MI groups.

7 and 14 (data not shown). Therefore, in the early phases after myocardial injury, CTSL likely played an important role in coordinating and enabling cell mobilization into circulation, ultimately homing into ischaemic tissues to participate in repair and restore function.

3.6 CTSL deficiency diminished cytokine expression and local homing response

Granulocyte-colony stimulating factor (G-CSF), stem cell factor (SCF), and stromal cell-derived factor-1 (SDF-1α) were significantly increased after MI in $Ctsl^{+/+}$ mice. However, $Ctsl^{-/-}$ mice showed significantly diminished levels of these cytokines at 55.1, 56 ($P < 0.05$), and 80% of $Ctsl^{+/+}$ mice, respectively (*Figure 4A*) when compared 3 days post-MI. As these cytokines are also homing signals for inflammatory cells, immunostaining further elucidated the differences in local myocardial inflammatory infiltration. *Figure 4B*(a) depicts representative immunohistochemistry images of heart sections from $Ctsl^{+/+}$ and $Ctsl^{-/-}$ mice stained for Mac3 and *c-kit*$^{+}$ ligands and indicated a diminished macrophage and *c-kit*$^{+}$ cell infiltration. Compared with $Ctsl^{+/+}$ mice, they indicate diminished homing of macrophages (by 58%) and c-kit^{+} cells (by 60%) in $Ctsl^{-/-}$ mice at day 3 post-MI ($P < 0.001$; *Figure 4B*(b)).

3.7 CTSL deficiency diminished myofibroblast population and proliferation, and impaired collagen & elastin deposition in the infarct scar

Myofibroblasts are the key cell population participating in the formation of the infarct scar. To further determine the mechanism of poor scar healing in $Ctsl^{-/-}$ mice post-MI, immunostaining for α-SMA-positive (SMA^{+}) myofibroblasts was used to determine the response of the myofibroblasts in the infarcted myocardium. As shown in *Figure 5A*, at the infarct zone in the $Ctsl^{+/+}$ mice, myofibroblasts first appeared by day 3, dominated at day 7, and remained abundant to day 14. However, $Ctsl^{-/-}$ mice showed a significantly reduced SMA^{+} cell population at 48, 77, and 50% of $Ctsl^{+/+}$ mice on days 3, 7, and 14, respectively ($P < 0.001$; *Figure 5B*). To further determine whether CTSL deficiency impaired myofibroblast proliferation,

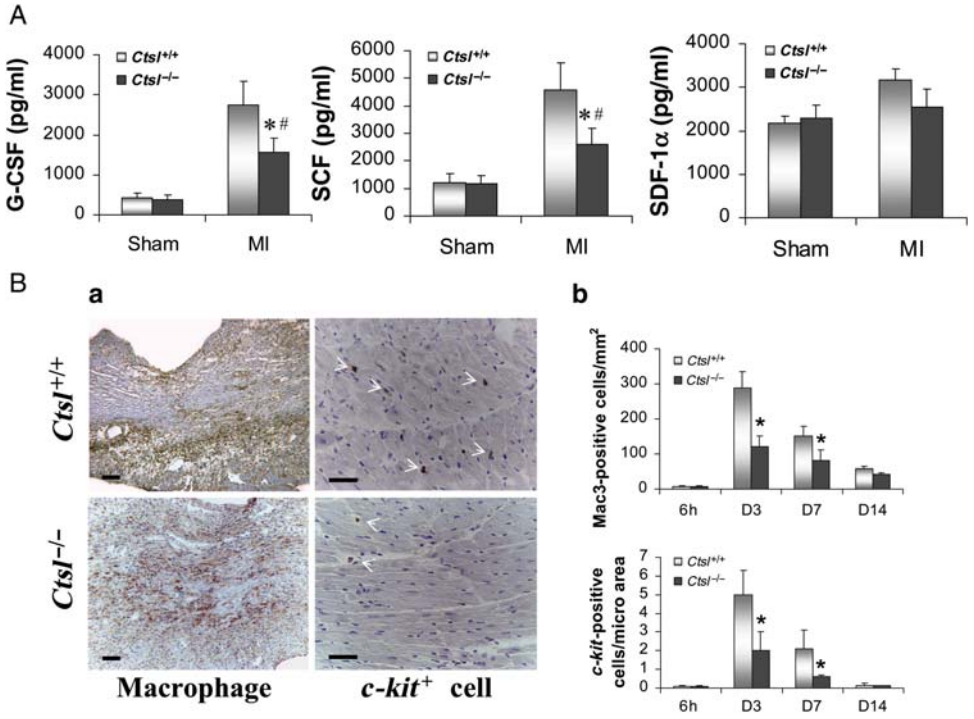

Figure 4 (*A*) Alterations in G-CSF, SCF, and SDF-1α levels in infracted myocardium post-MI. $^{*}P < 0.05$ vs. $Ctsl^{+/+}$ MI; $^{\#}P < 0.001$ vs. sham; (*B*) (a) Representative immunostaining for cardiac macrophage and c-kit^{+} in the infarct myocardium of $Ctsl^{+/+}$ and $Ctsl^{-/-}$ 3 days after MI. Scale bars represented 50 μm. (b) Quantification of time course macrophage and c-kit^{+} cells in infarcted myocardium after MI. $^{*}P < 0.001$ vs. $Ctsl^{+/+}$ groups ($n = 5$ for each group).

SMA^{+}/$Ki67^{+}$ dual positive cells were quantified at day 3 post-MI (*Figure 5A*(d and h)). A 49.8% reduction in the number of SMA^{+}/$Ki67^{+}$ cells was found in the border zone of $Ctsl^{-/-}$ mice at day 3 compared with $Ctsl^{+/+}$ mice (*Figure 5B*). Thus, impaired myofibroblast response and proliferation in the infarct myocardium further impaired scar collagen and elastin deposition. As shown in *Figure 5C*, Movat staining demonstrated loose densities of collagen, thinner scar, and less elastin deposition in $Ctsl^{-/-}$ mice (*Figure 5C*(d–f)). Quantitative collagen deposition in the infarct scar was significantly less when compared with $Ctsl^{+/+}$ mice as well ($P < 0.001$; *Figure 5D*). Thus, impaired myofibroblast response and proliferation is likely one of the factors that contribute to poor scar formation in $Ctsl^{-/-}$ mice.

3.8 CTSL deficiency impaired infarcted myocardium blood vessels formation

As shown in *Figure 6A*, western blot analysis showed that endothelial vascular endothelial growth factor (VEGF) was enhanced in infarcted border region after MI in $Ctsl^{+/+}$ mice. However, $Ctsl^{-/-}$ mice showed significantly diminished levels of 52% when compared with $Ctsl^{+/+}$ 3 days post-MI. *Figure 6B* showed the immunohistochemistry localized CD31 primarily to endothelial cells. At day 7 after MI, new vessels within the peri-infarct were strongly stained for CD31. Compared with $Ctsl^{+/+}$ mice, the capillary density was significantly less, especially in the infarct border region of $Ctsl^{-/-}$ mice. Quantitative capillary areas in the border zone are shown in *Figure 6C*. To further determine the fraction of proliferating endothelial cells in the infarcted myocardium, immunofluorescence for $CD31^{+}$/ $Ki67^{+}$ double-positive cells (*Figure 6B*(c and f)) were counted per microscopic field as shown in *Figure 6C*. Endothelial cell proliferation was noted to be significantly lower in number in $Ctsl^{-/-}$ mice when compared with that in $Ctsl^{+/+}$ mice ($P < 0.001$; *Figure 6C*); there was no difference in non-infarcted myocardium when compared with $Ctsl^{+/+}$ myocardium.

4. Discussion

Cardiac repair/remodelling following MI is a highly complex process, involving peripheral blood or bone marrow cell mobilization and homing, activation of diverse inflammatory and growth factor signalling pathways, cell proliferation and death, and extensive myofibroblasts, microvascular, and ECM remodelling.[24] Although the mechanisms are not fully elucidated, preventing ventricular dilatation and preserving functional improvement are keys in preventing progression of heart failure.

Cathepsins are cysteine proteases that participate in various types of tissue remodelling.[1,2] CTSL is known as a highly potent endoproteases of the cysteine cathepsin family and is ubiquitously expressed. Deficiency of CTSL in the heart primarily affects the lysosomal system, resulting in complex biochemical and cellular alterations which impair the structure and function of the lysosomal compartment in myocardium and contribute to spontaneously progressive DCM at aging.[18] We observed that CTSL activity was up-regulated after MI. In mice harbouring deficiency of the CTSL gene, the heart progressively dilated to congestive heart failure, associated with poor scar healing and doubling of the mortality post-MI when there was no gender differences in response to CTSL deletion. These findings suggest

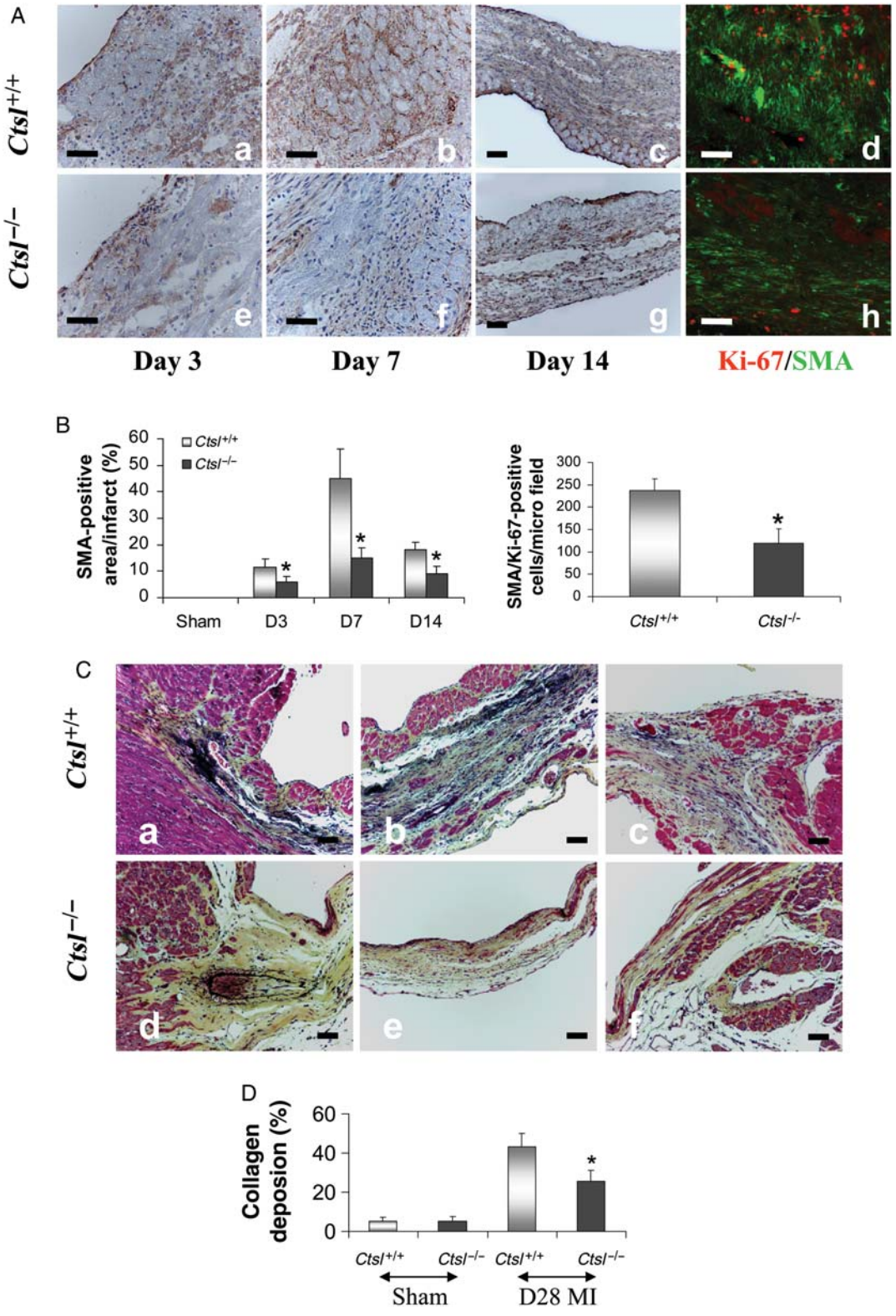

Figure 5 (*A*) Immunostaining for SMA in infarcted myocardium of *Ctsl*$^{+/+}$ (a–c) and *Ctsl*$^{-/-}$ (e–g) mice at days 3 (a, e), 7 (b, f), and 14 (c, g) after MI. Immunofluoresence double staining (d, h) for SMA (green) and Ki-67 (red) representative myofibroblast proliferations in *Ctsl*$^{-/-}$ and *Ctsl*$^{+/+}$ mice infarct myocardium. (*B*) Quantitative SMA-positive areas in various groups and quantification of SMA/Ki-67-positive cells at day 3 in infarcted myocardium. *$P < 0.001$ vs. *Ctsl*$^{+/+}$ MI groups. (*C*) Movat staining for *Ctsl*$^{+/+}$ (a–c) and *Ctsl*$^{-/-}$ (d–f) representative collagen (yellow) and elastin (black) deposits in the infarct myocardium. Scale bars represented 50 μm ($n = 5$ for each group).

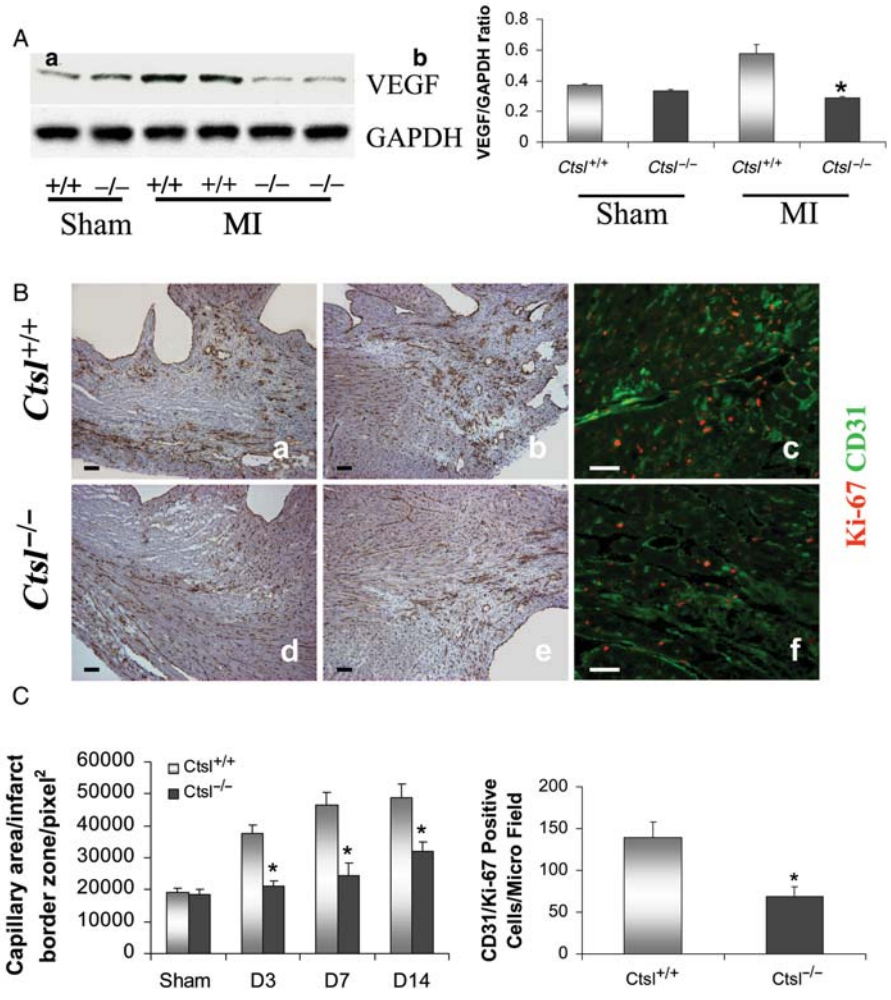

Figure 6 (*A*) (a) Western blot analysis for VEGF level at day 3 post-MI. (b) Quantification data of VEGF. *$P < 0.001$ vs. $Ctsl^{+/+}$ MI groups ($n = 4$) for each group. (*B*) Immunostaining for CD31 representative neovascularization in $Ctsl^{+/+}$ (a, b) and $Ctsl^{-/-}$ (d, e) mice. Immunofluoresence staining (c, f) represent CD31 (in green) and Ki67 (in red) at day 3 after MI. Orange colour indicates overlapping of CD31 and Ki69 staining. (*C*) Quantification data of capillary areas in infarct border zone at different time points after MI and CD31/Ki-67-positive cells number at day 3. *$P < 0.001$ vs. $Ctsl^{+/+}$ MI groups. Scale bars represented 50 μm ($n = 5$ for each group).

that CTSL is potentially one of the major coordinators for favourable repair and remodelling post-MI injury.

The present study suggested that myocardium injury caused early CTSL release and may correlate with the increase in bone marrow CTSL and MMP-9 activation. CTSL and MMP-9 activation in the myocardium and bone marrow suggests that part of MMP-9 activation is associated with CTSL. Mechanistically, this is plausible as activated CTSL can cleave pro-urokinase-type plasminogen activator (uPA) into the active form,[25] which in turn is a potent activator of MMPs.[26,27] On the other hand, inactive precursors of CTSL can also be activated by MMPs,[28] and thus complete the CTSL-uPA-MMP-CTSL positive feedback loop. Earlier increased CTSL are likely triggering MMP-9 activity contributing to the mobilization and recruitment of blood- or bone-marrow-derived accessory cells[29,30] that can home to the ischaemic myocardium at acute stage after MI to mediate repair and remodelling. During later stages, the source of CTSL and MMP-9 in the local infarcted myocardium is from neutrophil granules as we and Entman's lab have shown previously.[20,31] CTSL deficiency in contrast led to a relatively low MMP-9 level in local myocardium and bone marrow within 24 h of MI. This was associated with a significant impairment in recruitment of monocytes, natural killer cells, fibrocytes and *c-kit* positive cells in the peripheral circulation. This is consistent with earlier work by Urbich *et al.*[17] showing that CTSL play a role in the integration of circulating EPCs into ischaemic tissue. The local mobilization/homing signals G-CSF and SCF expression were also significantly diminished, and immunostaining of the injured myocardium confirmed decreased macrophage and *c-kit* positive cell homing post-MI to the myocardium in $Ctsl^{-/-}$ mice. Previous studies suggested that the homing action of these cells can be assisted by proteolytic enzymes, which degrades the ECM to allow cells to migrate efficiently to the site of injury.[29] Increasing evidence also confirms the importance of these mobilized cells in the cardiac repair and remodelling post-MI, particularly in neovascularization and tissue regeneration.[17,32–34]

One of the key cell types involved in rebuilding and remodelling following MI are the myofibroblasts, which play a central role in

fibrogenesis.[35] Myofibroblast-mediated scar contracture is required to avoid the progressive thinning and dilatation that are the substrates for heart failure.[36] Increased accumulation of these cells in infarct zones has been associated with favourable cardiac remodelling and improved cardiac function.[37–39] In addition, angiogenesis and granulation tissue formation are interlocking events in infarct repair[39,40] and myofibroblasts are important cellular mediators in this response. They produce VEGF[41] and endothelin,[42] and have been suggested in turn to contribute to blood vessel formation.[37,43,44] Previous studies indicate that the circulating fibrocytes contribute to the myofibroblast population in the wounded tissue originate from the bone marrow.[45,46] In this report, we evaluated whether a reduction in CTSL would impact fibrocyte mobilization and myofibroblast accumulation, thus contributing to cardiac dilatation and dysfunction. Indeed, the circulating fibrocyte population was significantly decreased in *Ctsl*$^{-/-}$ mice when compared with *Ctsl*$^{+/+}$ at day 3. Myofibroblast proliferation and accumulation were also diminished in the *Ctsl*$^{-/-}$ mice subjected to infarction. Thus, deficiency of CTSL impaired fibrocyte mobilization, contributed to reduced myofibroblast accumulation, local proliferation,[47] and scar stabilization, which required to maintain structural integrity of the injured myocardium, and lead to progression to heart failure and increased mortality between 7 and 28 days post-MI. On the other hand, myofibroblasts have both beneficial and adverse effect. They are required for scar formation to maintain the integrity of the heart following MI. However, extensive fibrosis may increased the stiffness of the heart and contribute to ventricular dysfunction.

Another important step in the wound-healing process is re-establishment of the capillary network, or angiogenesis. Angiogenesis is characterized by the invasion, migration, and proliferation of EPCs, endothelial cells, and smooth muscle cells. Decreased migration, infiltration, and proliferation of monocytes/macrophages, *c-kit* positive cells, and EPCs post-MI would reduce both indirect and direct angiogenesis.[48] In addition, CTSL is also encountered outside the cells or on the cell membrane[49] and can contribute to angiogenesis and recruitment of EPCs into the angiogenic region.[17] Recent studies demonstrated that CTSL and other cathepsins are highly expressed in various tumour cells and that inhibition of cathepsin activity reduced tumour vascularization and vascular branching.[9] Urbich *et al*. have reported that EPCs express high levels of CTSL which is essential for matrix degradation and invasion *in vitro*. Of important note, progenitor cells lacking CTSL do not home in to sites of ischaemia and do not augment neovascularization resulting impaired functional recovery following hind limb ischaemia.[17] In this study, angiogenesis after MI showed significant differences in the *Ctsl*$^{-/-}$ and *Ctsl*$^{+/+}$ mice. Deficiency of CTSL led to impairment in vascularization and significantly less capillary development in the infarct border zone at day 7 post-MI. Decreased endothelial cell proliferation was also observed in *Ctsl*$^{-/-}$ mice. VEGF is important in signalling proteins involved in angiogenesis. However, *Ctsl*$^{-/-}$ mice initially presented with a low level of VEGF which did not increase following MI. These data strengthen the fact that CTSL plays an essential role in angiogenesis during tissue repair, possibly through degradation of the vascular basement membrane and ECM, allowing progenitor cells to penetrate and home to injured area, enhance VEGF production and stimulates endothelial cell mitogenesis, cell migration, differentiation, and proliferation. These observations suggest CTSL contributes to angiogenesis in the infarct border zone as part of the remodelling process.

In this study, mice deficient in CTSL had a significantly impaired cardiac function after MI. This was accompanied by a diminished cell homing, impaired angiogenesis, and myofibroblast accumulation, leading to poor scar formation and cardiac dilatation. Thus, cardiac repair/remodelling benefits from activation of CTSL to improve remodelling and cardiac function after MI injury, and cathepsin L appear to be an important coordinator of the systemic response to cardiac injury.

Supplementary material

Supplementary material is available at *Cardiovascular Research* online.

Acknowledgements

Dr Liu is the Heart & Stroke/Polo Chair Professor of Medicine and Physiology, University of Toronto, and Scientific Director, Institute of Circulatory and Respiratory Health, Canadian Institutes of Health Research.

Conflict of interest: none declared.

Funding

This work was supported by grants from the Heart and Stroke Foundation of Ontario (T5651) and the Canadian Institutes of Health Research (CIHR) (MOP 494143).

References

1. Sam F, Siwik DA. Digesting the remodeled heart: role of lysosomal cysteine proteases in heart failure. Hypertension 2006;**48**:830–831.
2. Rajadurai M, Stanely Mainzen Prince P. Preventive effect of naringin on cardiac markers, electrocardiographic patterns and lysosomal hydrolases in normal and isoproterenol-induced myocardial infarction in Wistar rats. Toxicology 2007;**230**:178–188.
3. Liu Y, Li X, Peng D, Tan Z, Liu H, Qing Y *et al*. Usefulness of serum cathepsin L as an independent biomarker in patients with coronary heart disease. Am J Cardiol 2009;**103**:476–481.
4. Turski WA, Zaslonka J. Activity of cathepsin D and L in the heart muscle of coronary patients during coronary–aortal bypass graft operation. Med Sci Monit 2000;**6**:853–860.
5. Rawlings ND, Barrett AJ. MEROPS: the peptidase database. Nucleic Acids Res 2000;**28**:323–325.
6. Puente XS, Sanchez LM, Overall CM, Lopez-Otin C. Human and mouse proteases: a comparative genomic approach. Nat Rev Genet 2003;**4**:544–558.
7. Turk V, Turk B, Guncar G, Turk D, Kos J. Lysosomal cathepsins: structure, role in antigen processing and presentation, and cancer. Adv Enzyme Regul 2002;**42**:285–303.
8. Riese RJ, Mitchell RN, Villadangos JA, Shi GP, Palmer JT, Karp ER *et al*. Cathepsin S activity regulates antigen presentation and immunity. J Clin Invest 1998;**101**:2351–2363.
9. Yang Z, Cox JL. Cathepsin L increases invasion and migration of B16 melanoma. Cancer Cell Int 2007;**7**:8.
10. Wille A, Gerber A, Heimburg A, Reisenauer A, Peters C, Saftig P *et al*. Cathepsin L is involved in cathepsin D processing and regulation of apoptosis in A549 human lung epithelial cells. Biol Chem 2004;**385**:665–670.
11. Goulet B, Baruch A, Moon NS, Poirier M, Sansregret LL, Erickson A *et al*. A cathepsin L isoform that is devoid of a signal peptide localizes to the nucleus in S phase and processes the CDP/Cux transcription factor. Mol Cell 2004;**14**:207–219.
12. Bromme D, Kaleta J. Thiol-dependent cathepsins: pathophysiological implications and recent advances in inhibitor design. Curr Pharm Des 2002;**8**:1639–1658.
13. Roth W, Deussing J, Botchkarev VA, Pauly-Evers M, Saftig P, Hafner A *et al*. Cathepsin L deficiency as molecular defect of *furless*: hyperproliferation of keratinocytes and pertubation of hair follicle cycling. FASEB J 2000;**14**:2075–2086.
14. Honey K, Nakagawa T, Peters C, Rudensky A. Cathepsin L regulates CD4^{+} T cell selection independently of its effect on invariant chain: a role in the generation of positively selecting peptide ligands. J Exp Med 2002;**195**:1349–1358.
15. Nakagawa T, Roth W, Wong P, Nelson A, Farr A, Deussing J *et al*. Cathepsin L: critical role in Ii degradation and CD4 T cell selection in the thymus. Science 1998;**280**:450–453.

16. Stypmann J, Glaser K, Roth W, Tobin DJ, Petermann I, Matthias R *et al*. Dilated cardiomyopathy in mice deficient for the lysosomal cysteine peptidase cathepsin L. Proc Natl Acad Sci USA 2002;**99**:6234–6239.
17. Urbich C, Heeschen C, Aicher A, Sasaki K, Bruhl T, Farhadi MR *et al*. Cathepsin L is required for endothelial progenitor cell-induced neovascularization. Nat Med 2005; **11**:206–213.
18. Petermann I, Mayer C, Stypmann J, Biniossek ML, Tobin DJ, Engelen MA *et al*. Lysosomal, cytoskeletal, and metabolic alterations in cardiomyopathy of cathepsin L knockout mice. FASEB J 2006;**20**:1266–1268.
19. Spira D, Stypmann J, Tobin DJ, Petermann I, Mayer C, Hagemann S *et al*. Cell type-specific functions of the lysosomal protease cathepsin L in the heart. J Biol Chem 2007;**282**:37045–37052.
20. Sun M, Dawood F, Wen WH, Chen M, Dixon I, Kirshenbaum LA *et al*. Excessive tumor necrosis factor activation after infarction contributes to susceptibility of myocardial rupture and left ventricular dysfunction. Circulation 2004;**110**:3221–3228.
21. Sun M, Opavsky MA, Stewart DJ, Rabinovitch M, Dawood F, Wen WH *et al*. Temporal response and localization of integrins β1 and β3 in the heart after myocardial infarction: regulation by cytokines. Circulation 2003;**107**:1046–52.
22. Li GH, Shi Y, Chen Y, Sun M, Sader S, Maekawa Y *et al*. Gelsolin regulates cardiac remodeling after myocardial infarction through DNase I-mediated apoptosis. Circ Res 2009;**104**:896–904.
23. Sun M, Chen M, Dawood F, Zurawska U, Li JY, Parker T *et al*. Tumor necrosis factor-α mediates cardiac remodeling and ventricular dysfunction after pressure overload state. Circulation 2007;**115**:1398–1407.
24. Farahmand P, Lai TY, Weisel RD, Fazel S, Yau T, Menasche P *et al*. Skeletal myoblasts preserve remote matrix architecture and global function when implanted early or late after coronary ligation into infarcted or remote myocardium. Circulation 2008;**118**: S130–S137.
25. Schmitt M, Goretzki L, Janicke F, Calvete J, Eulitz M, Kobayashi H *et al*. Biological and clinical relevance of the urokinase-type plasminogen activator (uPA) in breast cancer. Biomed Biochim Acta 1991;**50**:731–741.
26. Ginestra A, Monea S, Seghezzi G, Dolo V, Nagase H, Mignatti P *et al*. Urokinase plasminogen activator and gelatinases are associated with membrane vesicles shed by human HT1080 fibrosarcoma cells. J Biol Chem 1997;**272**:17216–17222.
27. Heymans S, Luttun A, Nuyens D, Theilmeier G, Creemers E, Moons L *et al*. Inhibition of plasminogen activators or matrix metalloproteinases prevents cardiac rupture but impairs therapeutic angiogenesis and causes cardiac failure. Nat Med 1999;**5**: 1135–1142.
28. Jokimaa V, Oksjoki S, Kujari H, Vuorio E, Anttila L. Expression patterns of cathepsins B, H, K, L and S in the human endometrium. Mol Hum Reprod 2001;**7**:73–78.
29. Urbich C, Rossig L, Dimmeler S. Restoration of cardiac function with progenitor cells. Novartis Found Symp 2006;**274**:214–*223*; discussion 223–227, 272–276.
30. Cramer DE, Wagner S, Li B, Liu J, Hansen R, Reca R *et al*. Mobilization of hematopoietic progenitor cells by yeast-derived β-glucan requires activation of matrix metalloproteinase-9. Stem Cells 2008;**26**:1231–1240.
31. Lindsey M, Wedin K, Brown MD, Keller C, Evans AJ, Smolen J *et al*. Matrix-dependent mechanism of neutrophil-mediated release and activation of matrix metalloproteinase 9 in myocardial ischemia/reperfusion. Circulation 2001;**103**:2181–2187.
32. Orlic D, Kajstura J, Chimenti S, Jakoniuk I, Anderson SM, Li B *et al*. Bone marrow cells regenerate infarcted myocardium. Nature 2001;**410**:701–705.
33. Asahara T, Masuda H, Takahashi T, Kalka C, Pastore C, Silver M *et al*. Bone marrow origin of endothelial progenitor cells responsible for postnatal vasculogenesis in physiological and pathological neovascularization. Circ Res 1999;**85**:221–228.
34. Ayach BB, Yoshimitsu M, Dawood F, Sun M, Arab S, Chen M *et al*. Stem cell factor receptor induces progenitor and natural killer cell-mediated cardiac survival and repair after myocardial infarction. Proc Natl Acad Sci USA 2006;**103**:2304–2309.
35. Sun Y, Weber KT. Infarct scar: a dynamic tissue. Cardiovasc Res 2000;**46**:250–256.
36. Jugdutt BI. Ventricular remodeling after infarction and the extracellular collagen matrix: when is enough enough? Circulation 2003;**108**:1395–403.
37. Cimini M, Fazel S, Zhuo S, Xaymardan M, Fujii H, Weisel RD *et al*. c-Kit dysfunction impairs myocardial healing after infarction. Circulation 2007;**116**:I77–I82.
38. Okada H, Takemura G, Kosai K, Li Y, Takahashi T, Esaki M *et al*. Postinfarction gene therapy against transforming growth factor-β signal modulates infarct tissue dynamics and attenuates left ventricular remodeling and heart failure. Circulation 2005;**111**: 2430–2437.
39. Leor J, Rozen L, Zuloff-Shani A, Feinberg MS, Amsalem Y, Barbash IM *et al*. *Ex vivo* activated human macrophages improve healing, remodeling, and function of the infarcted heart. Circulation 2006;**114**:I94–I100.
40. Nian M, Lee P, Khaper N, Liu P. Inflammatory cytokines and postmyocardial infarction remodeling. Circ Res 2004;**94**:1543–1553.
41. Chintalgattu V, Nair DM, Katwa LC. Cardiac myofibroblasts: a novel source of vascular endothelial growth factor (VEGF) and its receptors Flt-1 and KDR. J Mol Cell Cardiol 2003;**35**:277–286.
42. Katwa LC. Cardiac myofibroblasts isolated from the site of myocardial infarction express endothelin *de novo*. Am J Physiol Heart Circ Physiol 2003;**285**: H1132–H1139.
43. Grunewald M, Avraham I, Dor Y, Bachar-Lustig E, Itin A, Jung S *et al*. VEGF-induced adult neovascularization: recruitment, retention, and role of accessory cells. Cell 2006;**124**:175–189.
44. Carmeliet P, Luttun A. The emerging role of the bone marrow-derived stem cells in (therapeutic) angiogenesis. Thromb Haemost 2001;**86**:289–297.
45. Mori L, Bellini A, Stacey MA, Schmidt M, Mattoli S. Fibrocytes contribute to the myofibroblast population in wounded skin and originate from the bone marrow. Exp Cell Res 2005;**304**:81–90.
46. El-Asrar AM, Missotten L, Geboes K. Expression of cyclo-oxygenase-2 and downstream enzymes in diabetic fibrovascular epiretinal membranes. Br J Ophthalmol 2008;**92**:1534–1539.
47. van Amerongen MJ, Bou-Gharios G, Popa E, van Ark J, Petersen AH, van Dam GM *et al*. Bone marrow-derived myofibroblasts contribute functionally to scar formation after myocardial infarction. J Pathol 2008;**214**:377–386.
48. Polverini PJ. Role of the macrophage in angiogenesis-dependent diseases. EXS 1997; **79**:11–28.
49. Rao JS. Molecular mechanisms of glioma invasiveness: the role of proteases. Nat Rev Cancer 2003;**3**:489–501.